

## HH Model

$$C \frac{dV}{dt} = I_{ext} - G_{Na}(V - E_{Na}) - G_K(V - E_K) - G_{leak}(V - E_{leak})$$

$$G_{Na} = \bar{G}_{Na} m^3 h \quad G_K = \bar{G}_K n^4$$

$$\frac{dm}{dt} = \frac{m_{\infty}(V) - m}{\tau_m(V)} \quad \frac{dh}{dt} = \frac{h_{\infty}(V) - h}{\tau_h(V)}$$

$$\frac{dn}{dt} = \frac{n_{\infty}(V) - n}{\tau_n(V)}$$

To obtain a constant steady-state membrane potential ( $dV/dt = 0$ ), there must be zero total current:

$$I_{total} = I_K + I_{Na} + I_{Cl} = 0$$

Substituting three current-voltage equations from the previous slide into the equation above and rearranging gives the Goldman-Hodgkin-Katz (GHK) constant-field equation (for the equations here, permeability  $P$  is just mobility  $u$ ).

$$\Delta V = \frac{RT}{F} \ln \frac{P_K K_o + P_{Na} Na_o + P_{Cl} Cl_i}{P_K K_i + P_{Na} Na_i + P_{Cl} Cl_o}$$

The varieties of potassium channels (some of them):

- Voltage gated** –  $K_v$  like the delayed rectifier of the HH model. Some of these also have inactivation gates. These repolarize action potentials and limit the spiking rate during excitation.
- Calcium dependent** –  $K(Ca)$  There are two varieties of these:
  - BK – gated by both  $V$  and  $Ca$ . Important for repolarization and for activity-dependent sensing.
  - SK – gated by  $Ca$  only. Produce afterhyperpolarization (AHP) and help govern stability after bouts of activity (e.g. between bursts).
- H channels** – non-specific channels that are related to K channels. These have only an inactivation gate.
- Inward rectifier** – Non-V-gated channels whose conductance is often controlled by intracellular second messengers.
- Tandem pore domain** – contribute to the resting potential.

Varities of calcium channels:

L-type – high threshold ( $>30$  mV), slow V inactivation,  $Ca^{++}$  inactivation.

P/Q, N, R – high threshold ( $>20$  mV), weak V inactivation,  $Ca^{++}$  inactivation.

T-type – low threshold ( $>70$  mV), strong V inactivation, no  $Ca^{++}$  inactivation.

These types were originally identified on voltage-clamp criteria, but have subsequently been associated with specific genes, with multiple genes for each type. They differ in pharmacology and in their localization.

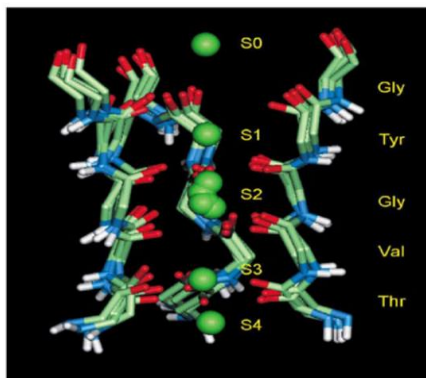
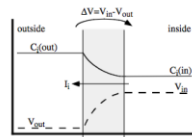


Fig. 5. Potassium ions in the selectivity filter as seen in the same simulation discussed in Fig. 4. Four snapshots from the simulation are superimposed, showing the filter regions of three of the four subunits, and the  $K^+$  ions (green spheres) that occupy (at different times) sites S0 to S4.

To illustrate a simple form of steady state, begin with the current-voltage equation derived in class from the Nernst-Planck equation with the constant field assumptions:

Steady state flux  
Independent fluxes  
Stirred bounding solutions  
Constant electric field in the membrane



$$I_i = \frac{(z_i F)^2 u_i}{d} \Delta V \frac{[C_i(d) e^{z_i F \Delta V / RT} - C_i(0)]}{e^{z_i F \Delta V / RT} - 1}$$

Thus, a more accurate steady-state model has to consider both active and passive transport, e.g. for potassium

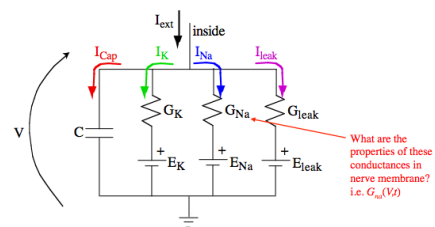
$$\frac{dK_{Na}}{dt} = \frac{A_{eff}}{F V_{cell}} [-I_{KNa}(\Delta V, K) - I_{KNaKATPase}(\Delta V, K, Na) - I_{KNaKCC}(\Delta V, K, Cl)]$$

e.g. GHK equation, passive transport      active transport due to Na-KATPase and KCC cotransporter

The membrane model (parallel currents through all the channels present):

$$I_{cap} + I_K + I_{Na} + I_{leak} = I_{ext}$$

$$C \frac{dV}{dt} = I_{ext} - G_K(V - E_K) - G_{Na}(V - E_{Na}) - G_{leak}(V - E_{leak})$$



## 1. Equilibrium

Free energy (equal at equil)

Equilibrium is defined as

Nernst Equation

$$\mu_i = \mu_i^o + RT \ln C_i + z_i F V$$

$$\Delta G = 0 \text{ or } \mu_i^1 = \mu_i^2$$

$$E = \frac{RT}{zF} \ln \frac{C_i}{C_o}$$

## 2. Ion Flux

Nernst-Planck Equation

GHK Equation

Rate Constants  
Flux Across Barrier

$$J = -uC \left[ RT \frac{d \ln C}{dx} + zF \frac{dV}{dx} \right]$$

$$I = -zF u C \left[ RT \frac{d \ln C}{dx} + zF \frac{dV}{dx} \right]$$

$$I_i = \frac{(z_i F)^2 u_i}{d} \Delta V \frac{C_i(d) e^{\frac{z_i F \Delta V}{RT}} - C_i(0)}{e^{\frac{z_i F \Delta V}{RT}} - 1}$$

$$\Delta V_{rest} = \frac{RT}{F} \ln \left( \frac{u_K K_o + u_{Na} Na_o + u_{Cl} Cl_i}{u_K K_i + u_{Na} Na_i + u_{Cl} Cl_o} \right)$$

$$k_i = (const) e^{\frac{-(G + \lambda z_i F \Delta V)}{RT}}$$

$$J_{AB} = k_i A, J_{BA} = k_{-i} B,$$

$$J = J_{AB} - J_{BA}$$

$$J = (const) e^{\frac{-(G + \lambda z_i F \Delta V)}{RT}} (A - B e^{\frac{z_i F \Delta V}{RT}})$$

$$\frac{RT}{F} = 26 mV$$

## 3. Phase Planes

Corelated Variables

State Vector

$$\text{Nullclines for MLE case } \dot{V} = 0 \rightarrow \omega = \frac{I_{ext} - G_{Ca} m_{\infty}(V - E_{Ca}) - \bar{G}_L(V - E_L)}{\bar{G}_K(V - E_K)}$$

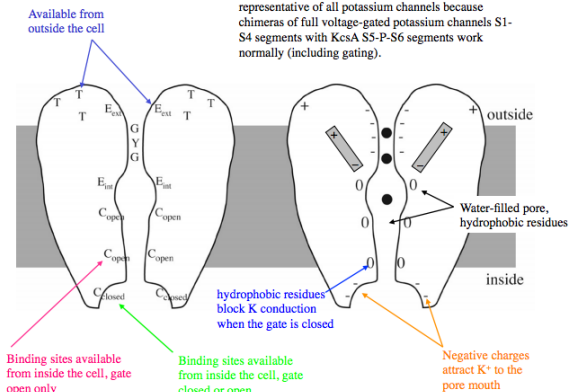
Jacobian

$$J = \begin{bmatrix} \frac{\partial F_1}{\partial x} & \frac{\partial F_1}{\partial y} \\ \frac{\partial F_2}{\partial x} & \frac{\partial F_2}{\partial y} \end{bmatrix} \Big|_{eq. pt.}$$

$$\dot{\omega} = 0 \rightarrow \omega = \omega_{\infty}(V)$$

$$\vec{x}(t) = \sum_{i=1}^N a_i \vec{e}_i e^{\lambda_i t}$$

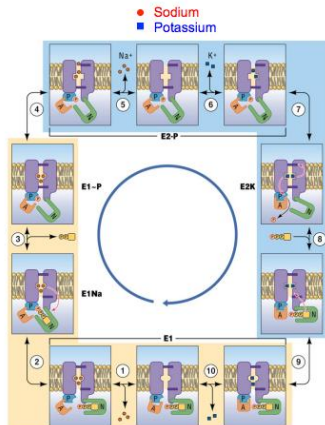
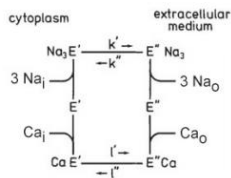
The structure of the KcsA channel is believed to be representative of all potassium channels because chimeras of full voltage-gated potassium channels S1-S4 segments with KcsA S5-S6 segments work normally (including gating).

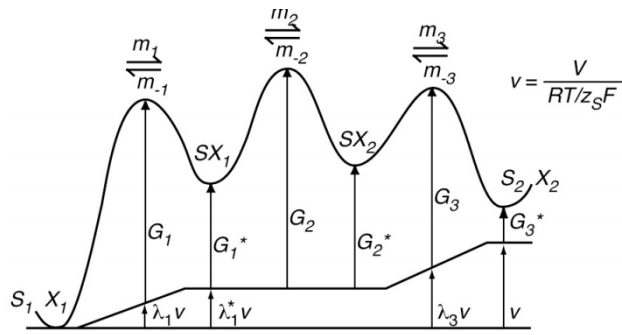


The sequence of steps in the Na-K ATPase is complex, involving separate transport of Na out, K in, and ATP cleavage.

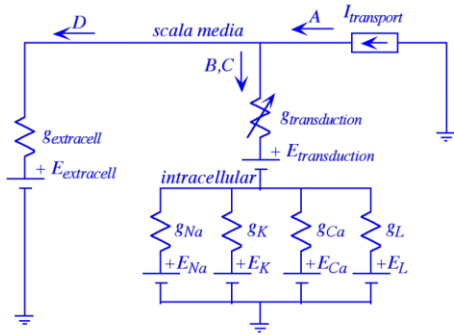
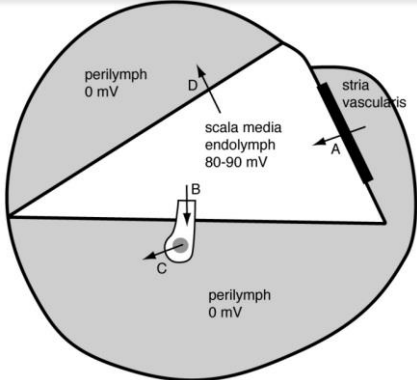
Note the gates (black) that occlude the Na and K during the transport step.

Motivated by this model Lauger and others have analyzed a slightly simpler transporter, the Na-Ca cotransporter with a similar scheme.





$$\begin{aligned}
 k_1 &= \alpha e^{-G_1/RT} & m_1 &= k_1 e^{-\lambda_1 v} & k_{-1} &= \alpha e^{-(G_1-G_1^*)/RT} & m_{-1} &= k_{-1} e^{-(\lambda_1-\lambda_1^*)v} \\
 k_2 &= \alpha e^{-(G_2-G_1^*)/RT} & m_2 &= k_2 & k_{-2} &= \alpha e^{-(G_2-G_2^*)/RT} & m_{-2} &= k_{-2} \\
 k_3 &= \alpha e^{-(G_3-G_2^*)/RT} & m_3 &= k_3 e^{-(\lambda_3-\lambda_1^*)v} & k_{-3} &= \alpha e^{-(G_3-G_3^*)/RT} & m_{-3} &= k_{-3} e^{-(\lambda_3-1)v}
 \end{aligned}$$



## Problem 2

Consider the system defined by the following two equations. This is an approximation to the near-threshold region of a neuron model.

$$\begin{aligned}
 \frac{dx}{dt} &= -y + x^2 - 2 \\
 \frac{dy}{dt} &= -y + x
 \end{aligned}$$

**Part a)** The nullclines are

$$\begin{aligned}
 y_{x\text{nullcline}} &= x^2 - 2 \\
 y_{y\text{nullcline}} &= x
 \end{aligned}$$

and are plotted in the phase plane on the next page (blue and green lines). The equilibrium points, where  $y_{x\text{nullcline}} = y_{y\text{nullcline}}$ , are the solutions of

$$x^2 - x - 2 = 0$$

which are  $x = 2, y = 2$  and  $x = -1, y = -1$  for the two equilibrium points, orange dots in the phase plane. The phase plane also shows trajectory directions in detail. Of course, these are not expected as part of the test answer, although vectors showing the general directions of trajectories in the various regions defined by the nullclines should have been included.

**Part b)** The Jacobians at the two equilibrium points are

$$J = \begin{bmatrix} 2x & -1 \\ 1 & -1 \end{bmatrix} \quad J_1 = \begin{bmatrix} 4 & -1 \\ 1 & -1 \end{bmatrix} \quad J_2 = \begin{bmatrix} -2 & -1 \\ 1 & -1 \end{bmatrix}$$

Computing the eigenvalues as the roots of  $\det(J - \lambda I) = 0$  gives

**Part c)** From index theory, a limit cycle would have to encircle the stable equilibrium point and not the saddle. However the unstable manifold discussed above prevents that from occurring, since trajectories cannot cross in the phase plane. This same conclusion can also be drawn from a careful inspection of the trajectory directions (blue arrows), although one cannot be sure of such an argument.

**Part d)** The stable manifolds of the saddle separate the phase plane into two regions. All trajectories in the left hand one, which contains the stable equilibrium point, must end in the stable equilibrium because (1) trajectory directions are toward the equilibrium point (and not out of the phase plane) and (2) there is no limit cycle. With a computer, a few trial trajectories can be computed; these are shown on the phase plane below in red, supporting this conclusion.

